



兰州大学
LANZHOU UNIVERSITY

Production of high-spin ω_J/ρ_J ($J=2,3,4,5$) mesons in π^-p reactions

李亭彦

Based on arXiv: 2601.17730

In collaboration with 白紫跃 刘翔

第五届强子与重味物理理论与实验联合研讨会

石家庄 2026/03/30

outline

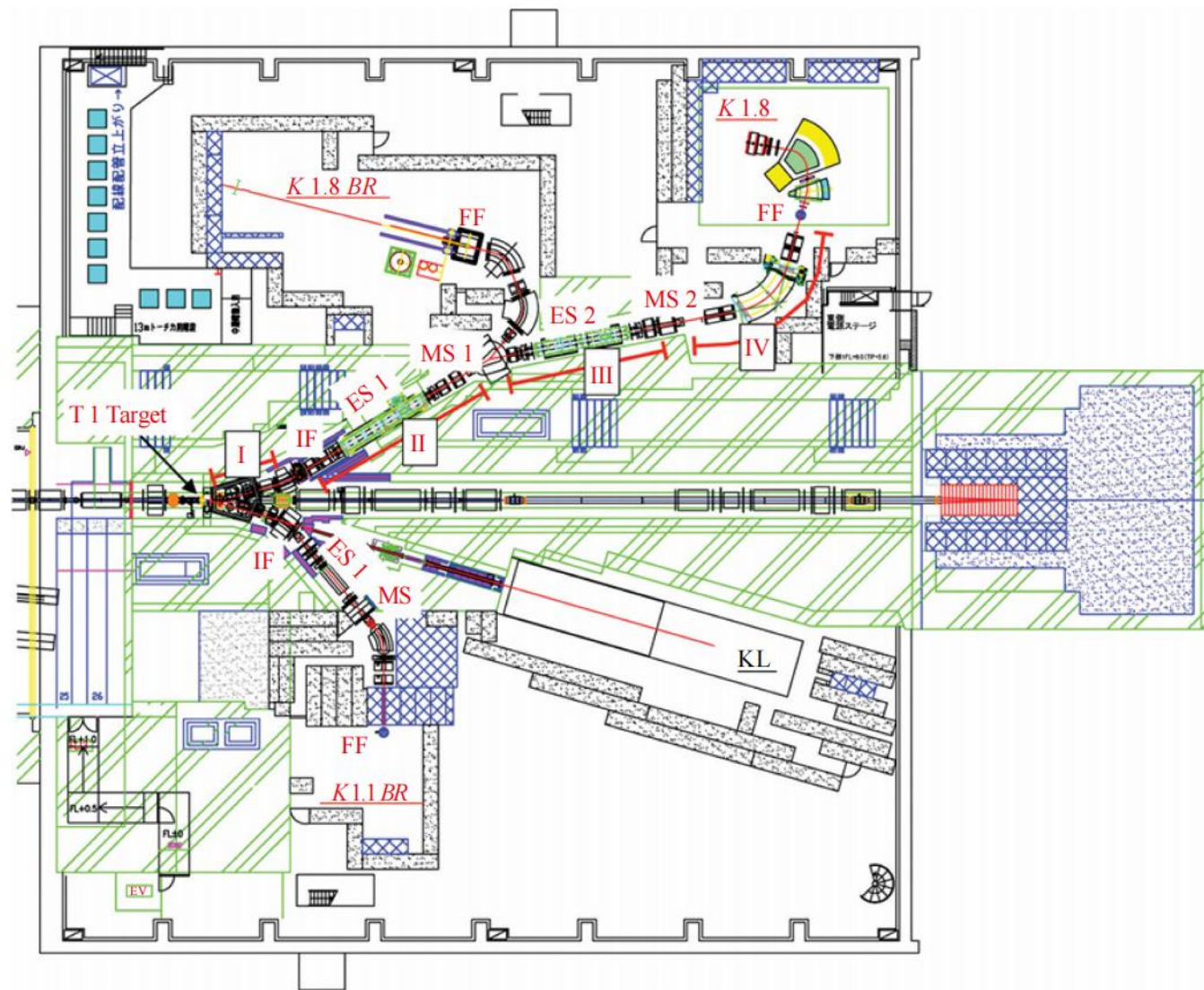
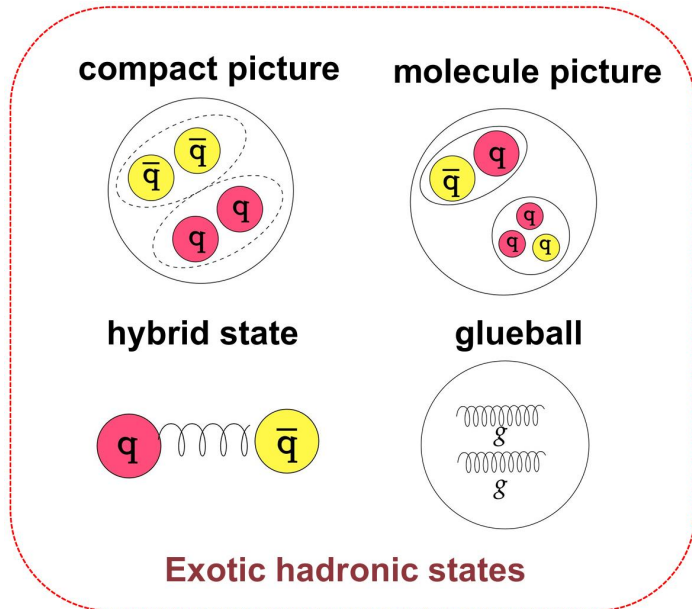
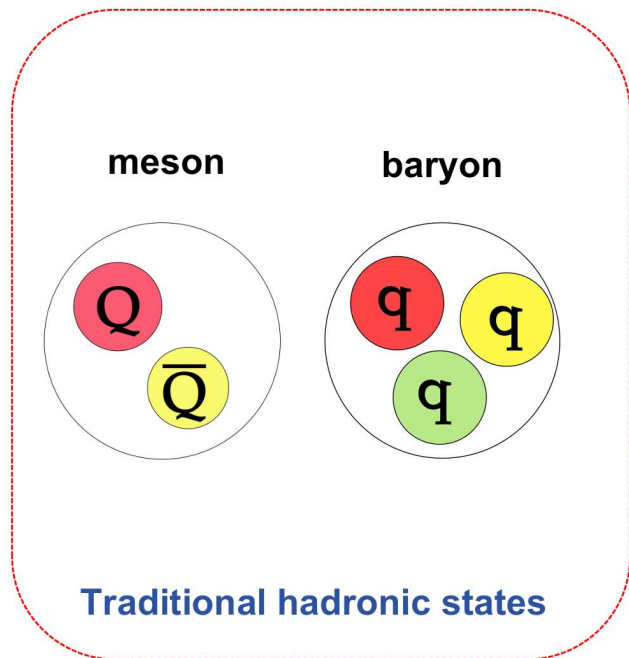
I. Background and Motivation

II. Theory framework

III. Numerical analysis

IV. Possible future prospect

Background: meson beam experiments



Layout diagrams of the Hadron Experimental Hall, charged secondary beamlines, and various experimental areas at J-PARC

Background: hadrons measured by meson beam experiments

➤ The energy region covers from a few tenths of a GeV to about 2 GeV.

η	0^-	✓	$\rho(1450)$	1^-		$\eta_2(1870)$	2^-	✓	$\rho_5(2350)$	5^-	✓
$f_0(500)$	0^+		$\eta(1475)$	0^-	✓	$\pi_2(1880)$	2^-	✓	$f_6(2510)$	6^+	✓
$\rho(770)$	1^-	✓	$f_0(1500)$	0^+	✓	$\rho(1900)$	1^-		$K_0^*(700)$	0^+	✓
$\omega(782)$	1^-	✓	$f_1(1510)$	1^+	✓	$f_2(1910)$	2^+	✓	$K^*(892)$	1^-	✓
$\eta'(958)$	0^-	✓	$f_2'(1525)$	2^+	✓	$a_0(1950)$	0^+		$K_1(1270)$	1^+	✓
$f_0(980)$	0^+	✓	$f_2(1565)$	2^+	✓	$f_2(1950)$	2^+	✓	$K_1(1400)$	1^+	✓
$a_0(980)$	0^+	✓	$\rho(1570)$	1^-	✓	$\rho_3(1990)$	3^-		$K^*(1410)$	1^-	✓
$\phi(1020)$	1^-	✓	$h_1(1595)$	1^+	✓	$\pi_2(2005)$	2^-	✓	$K_0^*(1430)$	0^+	✓
$h_1(1170)$	1^+	✓	$\pi_1(1600)$	1^-	✓	$f_2(2010)$	2^+	✓	$K_2^*(1430)$	2^+	✓
$b_1(1235)$	1^+	✓	$a_1(1640)$	1^+	✓	$f_0(2020)$	0^+	✓	$K(1460)$	0^-	✓
$a_1(1260)$	1^+	✓	$f_2(1640)$	2^+	✓	$a_4(2040)$	4^+	✓	$K_2(1580)$	2^-	✓
$f_2(1270)$	2^+	✓	$\eta_2(1645)$	2^-		$f_4(2050)$	4^+	✓	$K(1630)$?	✓
$f_1(1285)$	1^+	✓	$\omega(1650)$	1^-		$\pi_2(2100)$	2^-	✓	$K_1(1650)$	1^+	✓
$\eta(1295)$	0^-		$\omega_3(1670)$	3^-	✓	$f_0(2100)$	0^+		$K^*(1680)$	1^-	✓
$\pi(1300)$	0^-		$\pi_2(1670)$	2^-	✓	$f_2(2150)$	2^+		$K_2(1770)$	2^-	✓
$a_2(1320)$	2^+	✓	$\phi(1680)$	1^-		$\rho(2150)$	1^-		$K_3^*(1780)$	3^-	✓
$f_0(1370)$	0^+		$\rho_3(1690)$	3^-	✓	$\phi(2170)$	1^-		$K_2(1820)$	2^-	✓
$h_1(1380)$	1^+		$\rho(1700)$	1^-	✓	$f_0(2200)$	0^+	✓	$K(1830)$	0^-	✓

Low-spin

So many particles!

High-spin

Background: high spin states

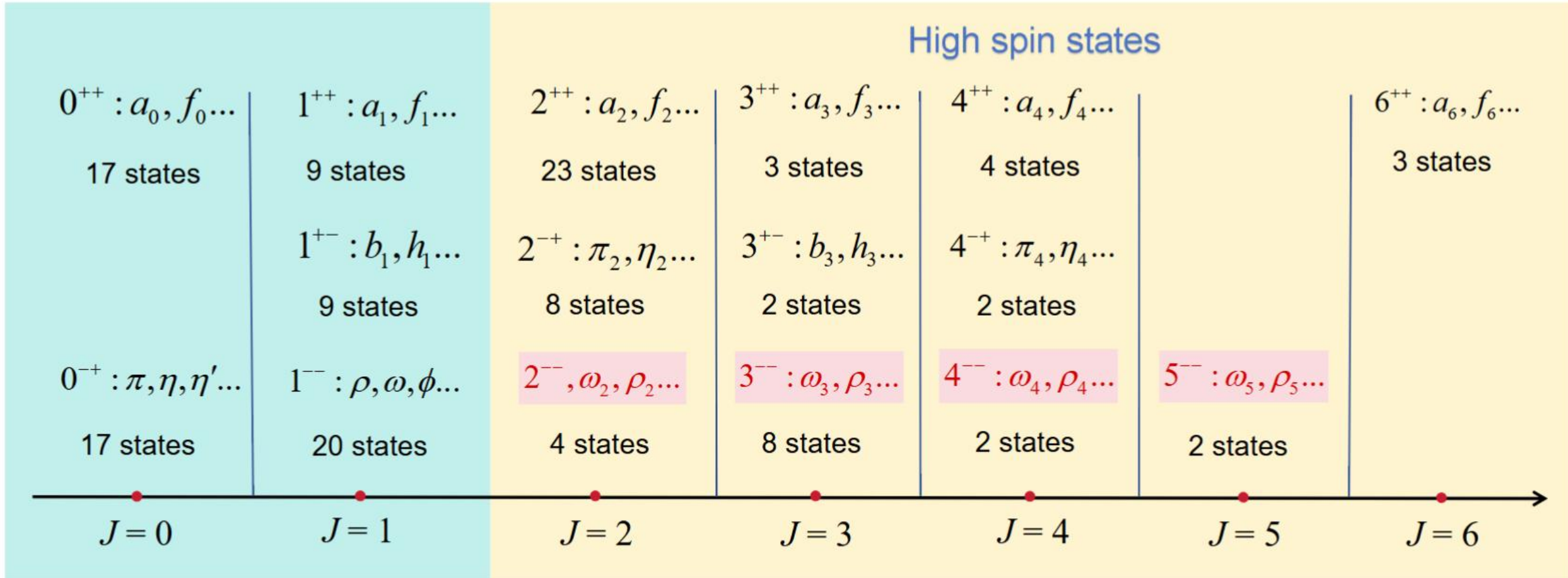
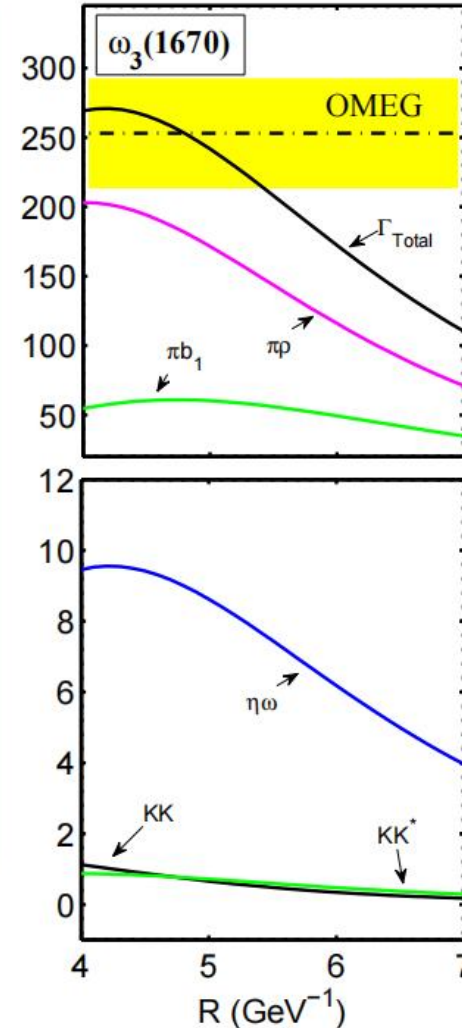
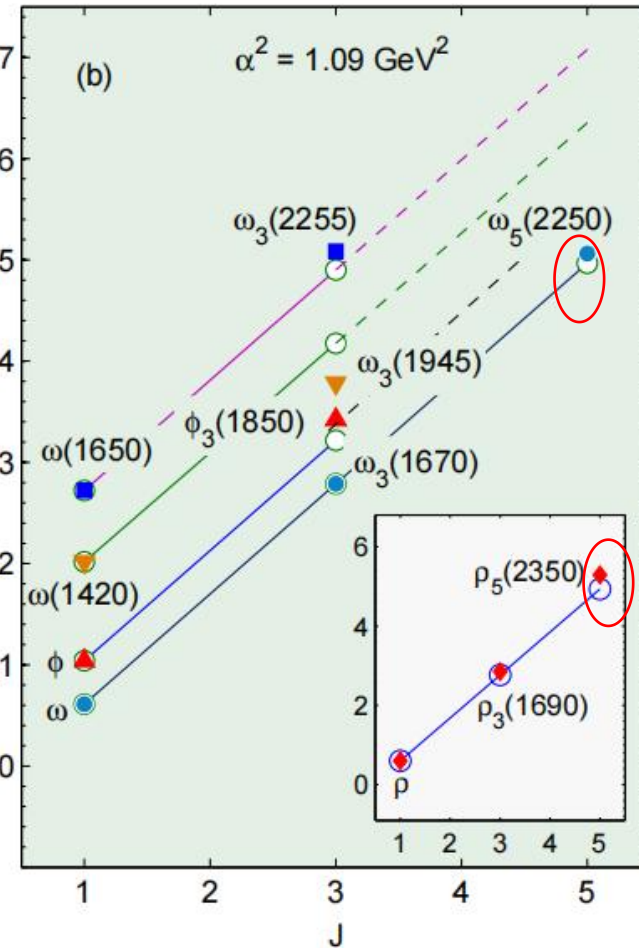
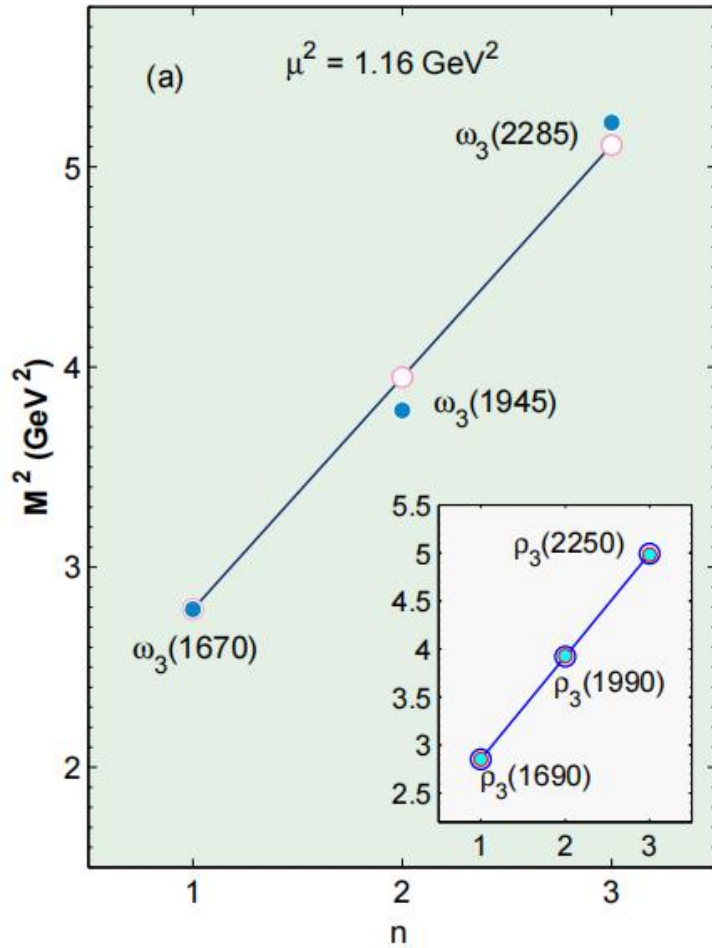


FIG. 1: A concise summary of light mesons [1].

Background: meson spectroscopy and strong decay for ω_J and ρ_J mesons



$\rho_3(1690), \Gamma_{exp.} = 190 \pm 40 \text{ [60]}$	
Channel	Value
Total	190
$\rho\rho$	105
$\pi\pi$	32.0
$\pi\omega$	23.1
πh_1	10.6
$a_2\pi$	8.07
$\eta\rho$	3.68
$a_1\pi$	3.26
KK	2.66

The establishment of the omega meson family remains to be improved

Motivation: meson beam experiments

- The production challenges of high-spin ω_J and ρ_J mesons remain to be explored and addressed.
- Considering the tree-level Feynman diagrams, can this process be adequately described?

3^{--}	$\omega_3(1670)$	$\rho_3(1690)$
	✓	✓
2^{--}	$\omega_2(1975)$	$\rho_4(2230)$
4^{--}	$\omega_4(2250)$	$\rho_4(2230)$
5^{--}	$\omega_5(2250)$	$\rho_5(2350)$

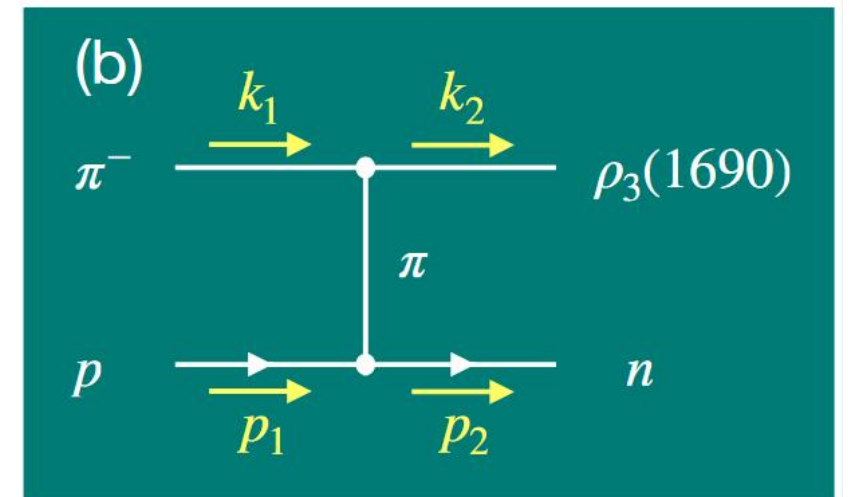
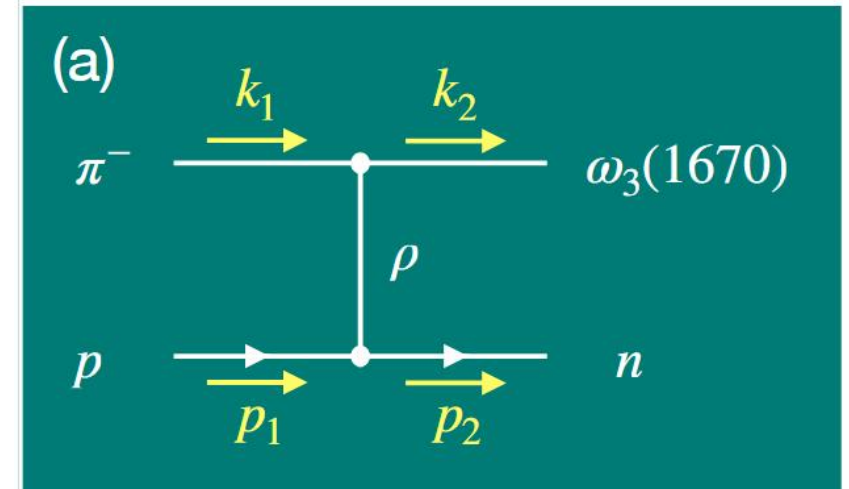
Nucl.Phys.B 138 (1978) 235-252

Phys.Rev.Lett. 32 (1974) 260-264

Phys.Rev.D 3 (1971) 2561-2572

Phys.Rev.Lett. 23 (1969) 146-149

Phys.Lett.B 26 (1968) 336-340



Theory framework: the effective Lagrangian approach

➤ $3 \times \bar{3}$ SU(3) flavor structure

$$P = \frac{1}{\sqrt{2}} \begin{pmatrix} \frac{\eta + \pi^0}{\sqrt{2}} & \pi^+ & K^+ \\ \pi^- & \frac{\eta_N - \pi^0}{\sqrt{2}} & K^0 \\ K^- & \bar{K}^0 & \eta \end{pmatrix},$$

$$V_1^\mu = \frac{1}{\sqrt{2}} \begin{pmatrix} \frac{\omega_1^\mu + \rho_1^{0\mu}}{\sqrt{2}} & \rho_1^{+\mu} & K_1^{*+\mu} \\ \rho_1^{-\mu} & \frac{\omega_1^\mu - \rho_1^{0\mu}}{\sqrt{2}} & K_1^{*0\mu} \\ K_1^{*-\mu} & \bar{K}_1^{*0\mu} & \omega_1^\mu \end{pmatrix},$$

$$A_1^\mu = \frac{1}{\sqrt{2}} \begin{pmatrix} \frac{f_1^\mu + a_1^{0\mu}}{\sqrt{2}} & a_1^{+\mu} & K_{1,A}^{+\mu} \\ a_1^{-\mu} & \frac{f_1^\mu - a_1^{0\mu}}{\sqrt{2}} & K_{1,A}^{0\mu} \\ K_{1,A}^{-\mu} & \bar{K}_{1,A}^{0\mu} & f_1^\mu \end{pmatrix}.$$

$$B_1^\mu = \frac{1}{\sqrt{2}} \begin{pmatrix} \frac{h_1^\mu + b_1^{0\mu}}{\sqrt{2}} & b_1^{+\mu} & K_{1,B}^{+\mu} \\ b_1^{-\mu} & \frac{h_1^\mu - b_1^{0\mu}}{\sqrt{2}} & K_{1,B}^{0\mu} \\ K_{1,B}^{-\mu} & \bar{K}_{1,B}^{0\mu} & h_1^\mu \end{pmatrix},$$

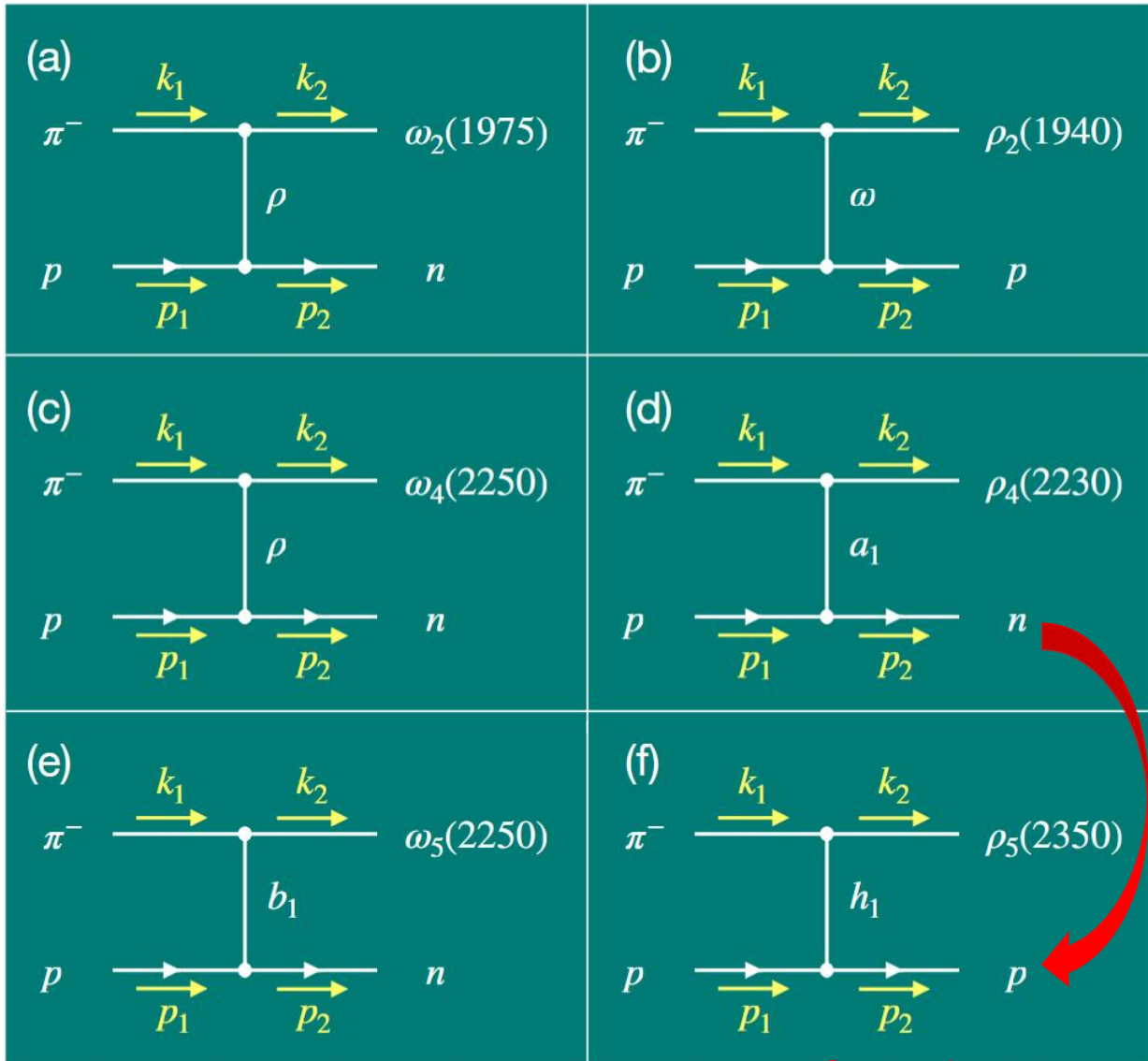
$$W_2^{\mu\nu} = \frac{1}{\sqrt{2}} \begin{pmatrix} \frac{\omega_2^{\mu\nu} + \rho_2^{0\mu\nu}}{\sqrt{2}} & \rho_2^{+\mu\nu} & K_2^{+\mu\nu} \\ \rho_2^{-\mu\nu} & \frac{\omega_2^{\mu\nu} - \rho_2^{0\mu\nu}}{\sqrt{2}} & K_2^{0\mu\nu} \\ K_2^{-\mu\nu} & \bar{K}_2^{0\mu\nu} & \omega_2^{\mu\nu} \end{pmatrix}$$

$$W_3^{\mu\nu\rho} = \frac{1}{\sqrt{2}} \begin{pmatrix} \frac{\omega_3^{\mu\nu\rho} + \rho_3^{0\mu\nu\rho}}{\sqrt{2}} & \rho_3^{+\mu\nu\rho} & K_3^{+\mu\nu\rho} \\ \rho_3^{-\mu\nu\rho} & \frac{\omega_3^{\mu\nu\rho} - \rho_3^{0\mu\nu\rho}}{\sqrt{2}} & K_3^{0\mu\nu\rho} \\ K_3^{-\mu\nu\rho} & \bar{K}_3^{0\mu\nu\rho} & \omega_3^{\mu\nu\rho} \end{pmatrix},$$

$$W_4^{\mu\nu\rho\sigma} = \frac{1}{\sqrt{2}} \begin{pmatrix} \frac{\omega_4^{\mu\nu\rho\sigma} + \rho_4^{0\mu\nu\rho\sigma}}{\sqrt{2}} & \rho_4^{+\mu\nu\rho\sigma} & K_4^{+\mu\nu\rho\sigma} \\ \rho_4^{-\mu\nu\rho\sigma} & \frac{\omega_4^{\mu\nu\rho\sigma} - \rho_4^{0\mu\nu\rho\sigma}}{\sqrt{2}} & K_4^{0\mu\nu\rho\sigma} \\ K_4^{-\mu\nu\rho\sigma} & \bar{K}_4^{0\mu\nu\rho\sigma} & \omega_4^{\mu\nu\rho\sigma} \end{pmatrix},$$

$$W_5^{\mu\nu\rho\sigma\gamma} = \frac{1}{\sqrt{2}} \begin{pmatrix} \frac{\omega_{5N}^{\mu\nu\rho\sigma\gamma} + \rho_5^{0\mu\nu\rho\sigma\gamma}}{\sqrt{2}} & \rho_5^{+\mu\nu\rho\sigma\gamma} & K_5^{+\mu\nu\rho\sigma\gamma} \\ \rho_5^{-\mu\nu\rho\sigma\gamma} & \frac{\omega_5^{\mu\nu\rho\sigma\gamma} - \rho_5^{0\mu\nu\rho\sigma\gamma}}{\sqrt{2}} & K_5^{0\mu\nu\rho\sigma\gamma} \\ K_5^{-\mu\nu\rho\sigma\gamma} & \bar{K}_5^{0\mu\nu\rho\sigma\gamma} & \omega_5^{\mu\nu\rho\sigma\gamma} \end{pmatrix}.$$

Theory framework: the effective Lagrangian approach



Isospin symmetry

$$\mathcal{L}_{\omega_2\rho\pi} = \frac{1}{2} g_{\omega_2\rho\pi} \omega_2^{\alpha\beta} \rho_\alpha^+ \partial_\beta \pi^-.$$

$$\mathcal{L}_{\rho NN} = g_{\rho NN} \bar{N} \gamma_\mu N \rho^\mu + \frac{f_{\rho NN}}{4M_p} \bar{N} \sigma_{\mu\nu} N (\partial^\mu \rho^\nu - \partial^\nu \rho^\mu),$$

$$\mathcal{L}_{\omega_4\rho\pi} = \frac{1}{2} g_{\omega_4\rho\pi} \omega_4^{\sigma\alpha\beta\gamma} \rho_\sigma^+ \partial_\alpha \partial_\beta \partial_\gamma \pi^-.$$

$$\mathcal{L}_{\rho_4 a_1 \pi} = \frac{1}{2} g_{\rho_4 a_1 \pi} \epsilon_{\mu\nu\rho\sigma} \rho_4^{\mu\alpha\beta\gamma} (\partial^\nu a_1^{\rho\sigma}) \partial_\alpha \partial_\beta \partial_\gamma \partial^\sigma \pi^-,$$

$$\mathcal{L}_{a_1 NN} = g_{a_1 NN} [\bar{N} \gamma_\mu \gamma_5 N] a_1^\mu + \frac{if_{a_1 NN}}{m_p} [\bar{N} \gamma_5 N] \partial_\mu a_1^\mu.$$

$$\mathcal{L}_{\omega_5 b_1 \pi} = \frac{1}{2} g_{\omega_5 b_1 \pi} \omega_5^{\sigma\alpha\beta\gamma\delta} b_{1,\sigma}^+ \partial_\alpha \partial_\beta \partial_\gamma \partial_\delta \pi^-.$$

$$\mathcal{L}_{b_1 NN} = \frac{if_B}{m_{b_1}} [\bar{N} \sigma_{\mu\nu} \gamma_5 N] \partial^\nu b_1^\mu.$$

$$\mathcal{L}_{\rho_5 h_1 \pi} = \frac{1}{2} g_{\rho_5 h_1 \pi} \rho_5^{\mu\alpha\beta\gamma\delta} h_{1,\mu} \partial_\alpha \partial_\beta \partial_\gamma \partial_\delta \pi^-.$$

FIG. 7: Feynman diagrams for the $\pi^- p \rightarrow \omega_J/\rho_J + N$ reactions.

Theory framework: the effective Lagrangian approach

➤ Feynman amplitude

$\pi^- p \rightarrow \omega_2(1975)n$ via t -channel ρ exchange:

$$i\mathcal{M}_{\omega_2} = -\frac{i}{2}g_{\omega_2\rho\pi}\varepsilon^{\alpha\beta*}(k_2)(k_{1\beta})\frac{-i(g_\alpha^\mu + q_\mu q_\alpha/m_\rho^2)}{t - m_\rho^2} \\ \times \bar{u}(p_2)\left(g_{\rho NN}\gamma_\mu + \frac{f_{\rho NN}}{2m_p}\gamma_\mu\not{q}\right)u(p_1)F_t(q),$$

$\pi^- p \rightarrow \rho_2(1940)p$ via t -channel ω exchange:

$$i\mathcal{M}_{\rho_2} = -\frac{i}{2}g_{\rho_2\omega\pi}\varepsilon^{\alpha\beta*}(k_2)(k_{1\beta})\frac{-i(g_\alpha^\mu + q_\mu q_\alpha/m_\omega^2)}{t - m_\omega^2} \\ \times \bar{u}(p_2)\left(g_{\omega NN}\gamma_\mu + \frac{f_{\omega NN}}{2m_p}\gamma_\mu\not{q}\right)u(p_1)F_t(q),$$

$$i\mathcal{M}_{\omega_3} = \frac{1}{2}g_{\omega_3\rho\pi}\varepsilon^{\mu\nu\rho\sigma}q_\nu k_1^\alpha k_1^\beta k_{1\sigma}\varepsilon_{\mu\alpha\beta}^*(k_2)\frac{-i(g_\rho^\xi + q^\xi q_\rho/m_\rho^2)}{t - m_\rho^2} \\ \times \bar{u}(p_2)\left(g_{\rho NN}\gamma_\xi + \frac{f_{\rho NN}}{2m_p}\gamma_\xi\not{q}\right)u(p_1)F_t(q), \quad (7)$$

$$i\mathcal{M}_{\rho_3} = -\frac{1}{2}g_{\rho_3\pi\pi}\frac{f_{\pi NN}}{m_\pi}\bar{u}(p_2)\gamma_\sigma\gamma_5u(p_1)q^\sigma\varepsilon_{\mu\nu\rho}^*(k_2) \\ \times (k_{1\mu}k_{1\nu}k_{1\rho} + q_\mu q_\nu q_\rho)\frac{i}{t - m_\pi^2}F_t(q),$$

$$F_t(q) = \left(\frac{\Lambda_t^2 - m^2}{\Lambda_t^2 - q^2}\right)^2, \quad \frac{1}{t - m_\pi^2} \rightarrow \left(\frac{s}{s_{scale}}\right)^{\alpha_\pi(t)} \frac{\pi\alpha'_\pi}{\Gamma[1 + \alpha_\pi(t)] \sin[\pi\alpha_\pi(t)]}, \quad \alpha_\pi(t) = 0.7(t - m_\pi^2), \quad <10/17>$$

Theory framework: the effective Lagrangian approach

➤ Feynman amplitude

$\pi^- p \rightarrow \omega_4(2250)n$ via t -channel ρ exchange:

$$i\mathcal{M}_{\omega_4} = \frac{i}{2} g_{\omega_4\rho\pi} k_{1\alpha} k_{1\beta} k_{1\gamma} \varepsilon^{\sigma\alpha\beta\gamma*}(k_2) \frac{-i(g_\sigma^\mu + q^\mu q_\sigma/m_\rho^2)}{t - m_\rho^2} \\ \times \bar{u}(p_2) \left[g_{\rho NN} \gamma_\mu + \frac{f_{\rho NN}}{2m_p} \gamma_\mu \not{q} \right] u(p_1) F_t(q),$$

$\pi^- p \rightarrow \rho_4(2230)n$ via t -channel a_1 exchange:

$$i\mathcal{M}_{\rho_4} = -\frac{1}{2} g_{\rho_4 a_1 \pi} \epsilon_{\mu\nu\rho\sigma} q^\nu k_{1\alpha} k_{1\beta} k_{1\gamma} k_1^\sigma \\ \varepsilon^{\mu\alpha\beta\gamma*}(k_2) \frac{-i(g_\rho^\xi + q^\xi q_\rho/m_{a_1}^2)}{t - m_{a_1}^2} F_t(q) \\ \times \bar{u}(p_2) \left(g_{a_1 NN} \gamma_\xi \gamma_5 - \frac{f_{a_1 NN}}{M_p} \gamma_5 \not{q} \right) u(p_1),$$

$\pi^- p \rightarrow \omega_5(2250)n$ via t -channel b_1 exchange:

$$i\mathcal{M}_{\omega_5} = \frac{1}{2} \frac{f_{b_1 NN}}{m_{b_1}} g_{\omega_5 b_1 \pi} k_{1\alpha} k_{1\beta} k_{1\gamma} k_{1\delta} \varepsilon^{\sigma\alpha\beta\gamma\delta*}(k_2) \\ \times \frac{-i(g_\sigma^\mu + q^\mu q_\sigma/m_{b_1}^2)}{t - m_{b_1}^2} \bar{u}(p_2) \sigma_{\mu\nu} \gamma_5 u(p_1) \\ \times q^\nu F_t(q),$$

$\pi^- p \rightarrow \rho_5(2350)n$ via t -channel h_1 exchange:

$$i\mathcal{M}_{\rho_5} = -\frac{1}{2} \frac{f_{h_1 NN}}{m_{b_1}} g_{\rho_5 h_1 \pi} k_{1\alpha} k_{1\beta} k_{1\gamma} k_{1\delta} \varepsilon^{\sigma\alpha\beta\gamma\delta*}(k_2) \\ \times \frac{-i(g_\sigma^\mu + q^\mu q_\sigma/m_{h_1}^2)}{t - m_{h_1}^2} \bar{u}(p_2) \sigma_{\mu\nu} \gamma_5 u(p_1) \\ \times q^\nu F_t(q).$$

$$\frac{1}{t - m_R^2} \rightarrow \left(\frac{s}{s_{scale}} \right)^{\alpha_R(t)-1} \frac{\pi \alpha'_R}{\Gamma[\alpha_R(t)] \sin[\pi \alpha_R(t)]}, \quad \alpha_R(t) = 1 + \alpha'_R(t - m_R^2),$$

Theory framework: the effective Lagrangian approach

The differential cross section in the center-of-mass (c.m.) frame is given by

$$\frac{d\sigma}{d\cos\theta} = \frac{1}{32\pi s} \frac{|\vec{k}_2^{\text{c.m.}}|}{|\vec{k}_1^{\text{c.m.}}|} \left(\frac{1}{2} \sum_{\lambda} |\mathcal{M}|^2 \right),$$

The explicit expressions for the projection operators of fields from **spin-3 to spin-5** are given as follows

$$\Delta_{\alpha}^{\beta}(1, p) = -\bar{g}_{\alpha}^{\beta} = -\left(g_{\alpha}^{\beta} - \frac{1}{p^2} p_{\alpha} p^{\beta} \right). \quad \Delta_{\alpha_1 \alpha_2}^{\beta_1 \beta_2}(2, p) = \frac{1}{2} \left(\bar{g}_{\alpha_1}^{\beta_1} \bar{g}_{\alpha_2}^{\beta_2} + \bar{g}_{\alpha_1}^{\beta_2} \bar{g}_{\alpha_2}^{\beta_1} - \frac{2}{3} \bar{g}_{\alpha_1 \alpha_2} \bar{g}^{\beta_1 \beta_2} \right).$$

$$\Delta_{\alpha_1 \alpha_2 \alpha_3}^{\beta_1 \beta_2 \beta_3}(3, p) = -\frac{1}{36} \sum_{P(\alpha), P(\beta)} \left(\bar{g}_{\alpha_1}^{\beta_1} \bar{g}_{\alpha_2}^{\beta_2} \bar{g}_{\alpha_3}^{\beta_3} - \frac{3}{5} \bar{g}_{\alpha_1 \alpha_2} \bar{g}^{\beta_1 \beta_2} \bar{g}_{\alpha_3}^{\beta_3} \right) \quad \bar{g}_{\mu\nu} = g_{\mu\nu} - \frac{1}{p^2} p_{\mu} p_{\nu}.$$

$$\Delta_{\alpha_1 \alpha_2 \alpha_3 \alpha_4}^{\beta_1 \beta_2 \beta_3 \beta_4}(4, p) = \frac{1}{576} \sum_{P(\alpha), P(\beta)} \left(\bar{g}_{\alpha_1}^{\beta_1} \bar{g}_{\alpha_2}^{\beta_2} \bar{g}_{\alpha_3}^{\beta_3} \bar{g}_{\alpha_4}^{\beta_4} - \frac{6}{7} \bar{g}_{\alpha_1 \alpha_2} \bar{g}^{\beta_1 \beta_2} \bar{g}_{\alpha_3}^{\beta_3} \bar{g}_{\alpha_4}^{\beta_4} + \frac{3}{35} \bar{g}_{\alpha_1 \alpha_2} \bar{g}_{\alpha_3 \alpha_4} \bar{g}^{\beta_1 \beta_2} \bar{g}^{\beta_3 \beta_4} \right),$$

$$\Delta_{\alpha_1 \alpha_2 \alpha_3 \alpha_4 \alpha_5}^{\beta_1 \beta_2 \beta_3 \beta_4 \beta_5}(5, p) = -\left(\frac{1}{120} \right)^2 \sum_{P(\alpha), P(\beta)} \left(\bar{g}_{\alpha_1}^{\beta_1} \bar{g}_{\alpha_2}^{\beta_2} \bar{g}_{\alpha_3}^{\beta_3} \bar{g}_{\alpha_4}^{\beta_4} \bar{g}_{\alpha_5}^{\beta_5} - \frac{10}{9} \bar{g}_{\alpha_1 \alpha_2} \bar{g}^{\beta_1 \beta_2} \bar{g}_{\alpha_3}^{\beta_3} \bar{g}_{\alpha_4}^{\beta_4} \bar{g}_{\alpha_5}^{\beta_5} + \frac{5}{21} \bar{g}_{\alpha_1 \alpha_2} \bar{g}_{\alpha_3 \alpha_4} \bar{g}^{\beta_1 \beta_2} \bar{g}^{\beta_3 \beta_4} \bar{g}_{\alpha_5}^{\beta_5} \right),$$

Phys.Rev.D 111 (2025) 5, 054031

The propagator of a field for a boson field can be written as

$$S(p) = \frac{1}{p^2 - M^2} (\not{p} + M) \Delta_{\alpha_1 \dots \alpha_{n-1}}^{\beta_1 \dots \beta_{n-1}}(j, p).$$

Numerical analysis: the cross section of $\omega_3(1650)$ meson

- The fitted results
 - Left: the total cross section
 - Right: the different cross section

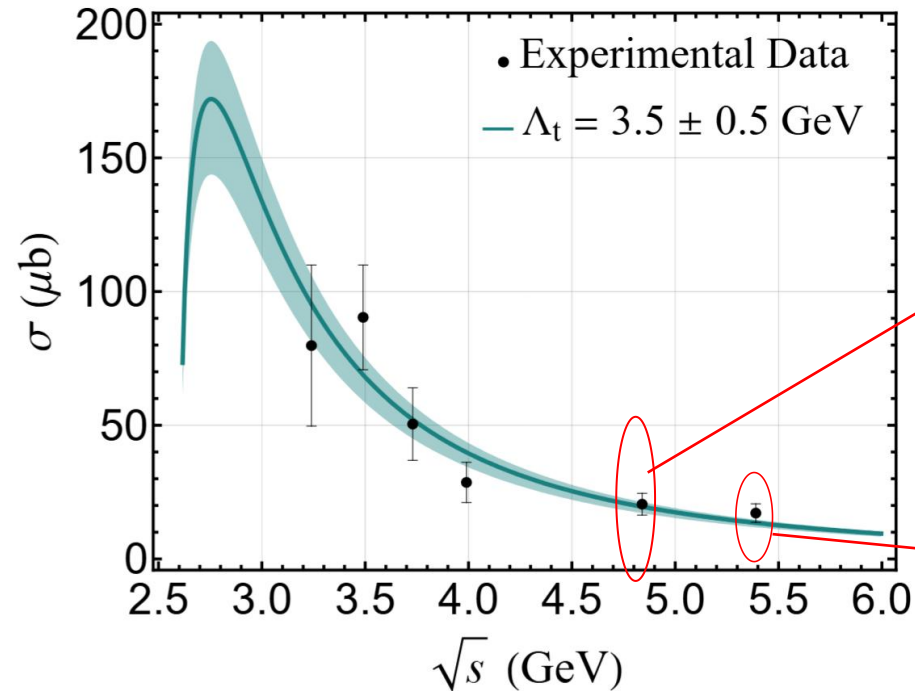


FIG. 3: The total cross section for the reaction $\pi^- p \rightarrow \omega_3(1670)n$. The black points with error bars correspond to the experimental data from Refs. [16, 17, 21–23].

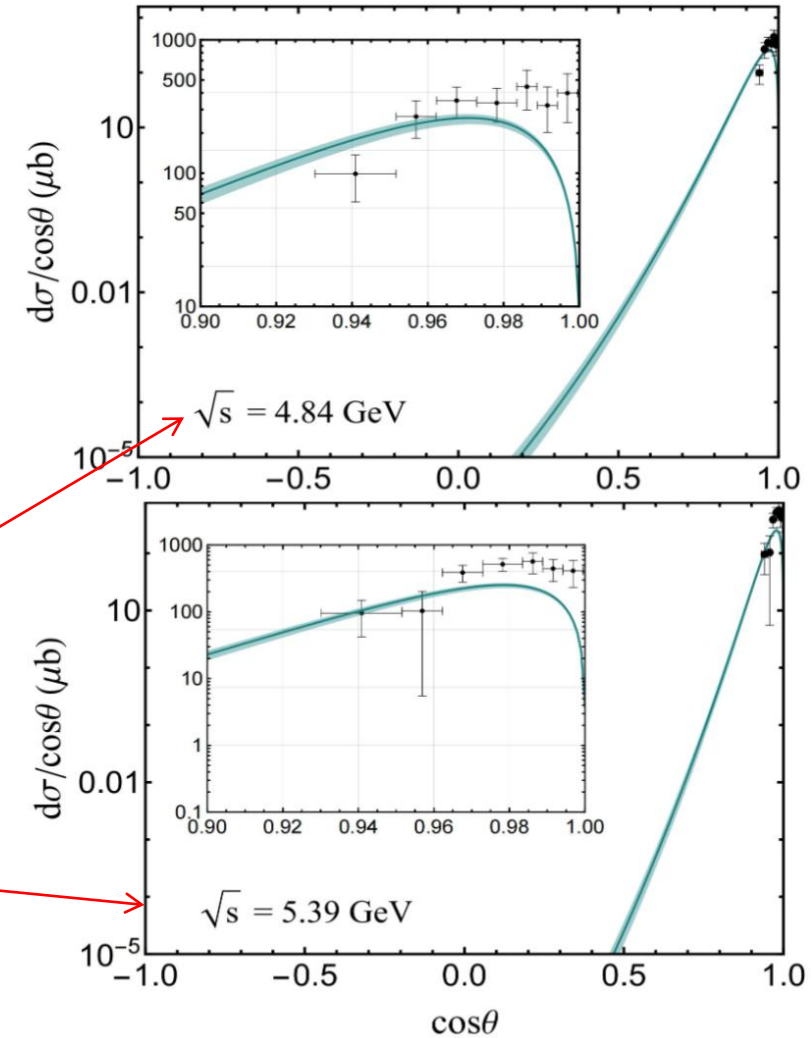


FIG. 4: The differential cross section $d\sigma/d\cos\theta$ of the $\omega_3(1670)$ production at different c.m. energy E_{cm} . The black points with error bars correspond to the experimental data from Ref. [17].

Numerical analysis: the cross section of the $\rho_3(1690)$ meson

- The fitted results
 - Left: the total cross section
 - Right: the different cross section

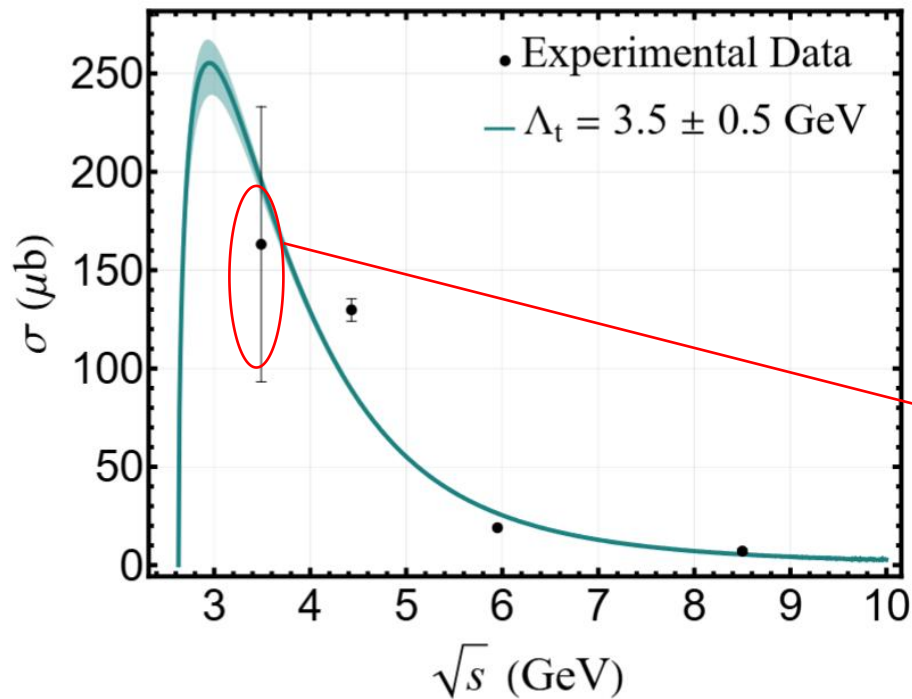


FIG. 5: The total cross section for the reaction $\pi^- p \rightarrow \rho_3(1690)n$. The black points with error bars correspond to the experimental data from Refs. [18, 24–26].

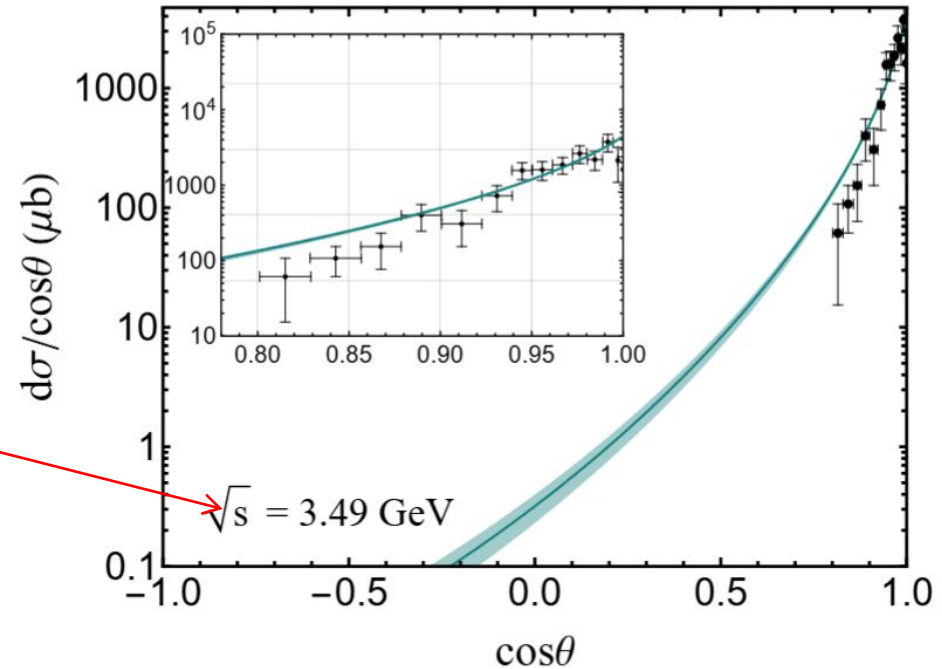


FIG. 6: The differential cross section $d\sigma/d\cos\theta$ of the $\rho_3(1690)$ production at c.m. energy $E_{cm} = 3.49$ GeV. The black points with error bars correspond to the experimental data from Ref. [18].

Numerical analysis: the total cross section of the

$\omega_2(1975)$, $\rho_2(1940)$, $\omega_4(2250)$, $\rho_4(2230)$, $\omega_5(2250)$, $\rho_5(2350)$

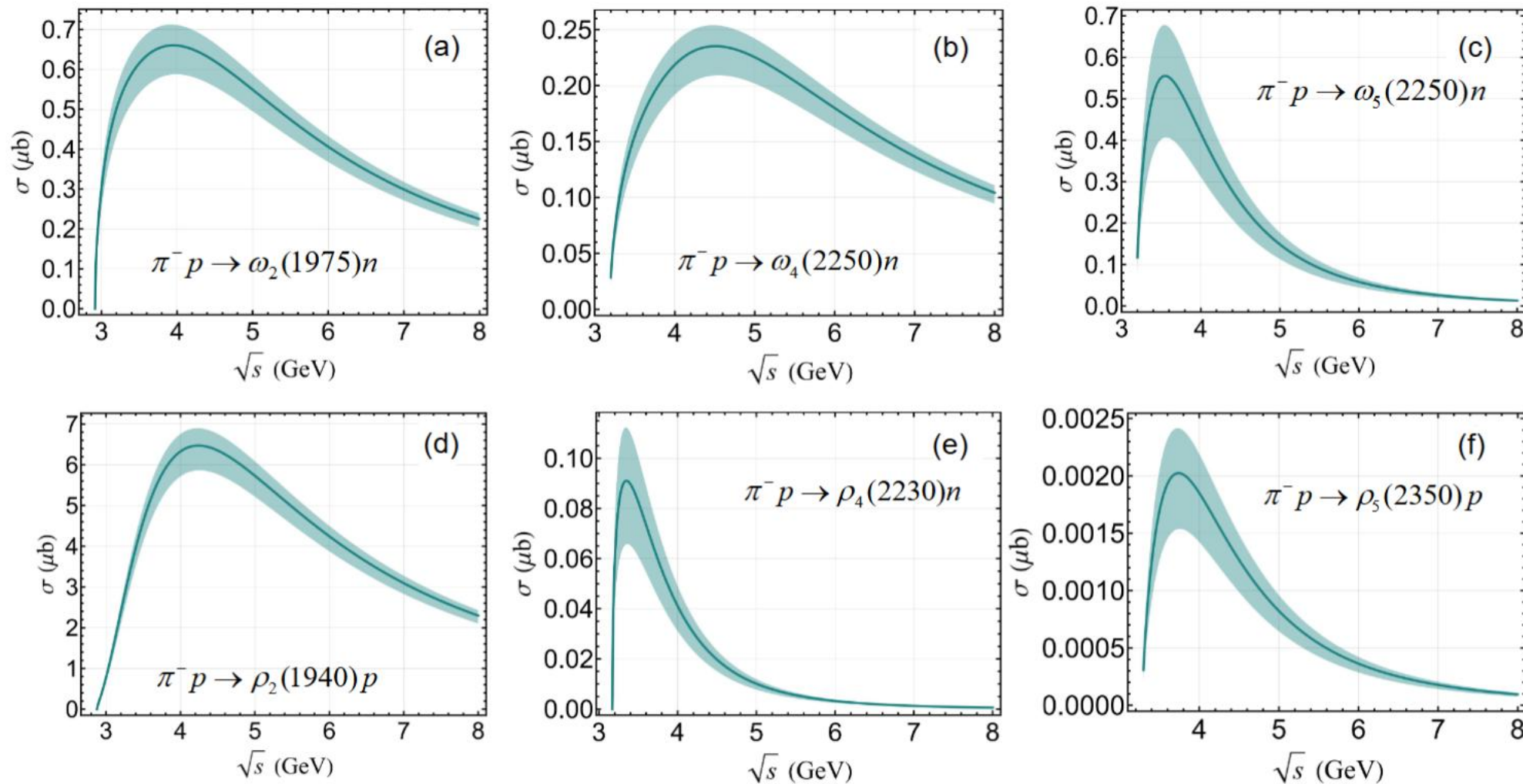


FIG. 8: The energy dependence of the total cross section for production of the $\omega_2(1975)$, $\rho_2(1940)$, $\omega_4(2250)$, $\rho_4(2230)$, $\omega_5(2250)$, $\rho_5(2350)$ through t -channel with cutoff $\Lambda_t = 3.5 \pm 0.5$ GeV. <15 / 17>

Numerical analysis: the different cross section of the $\omega_2(1975)$, $\rho_2(1940)$, $\omega_4(2250)$, $\rho_4(2230)$, $\omega_5(2250)$, $\rho_5(2350)$

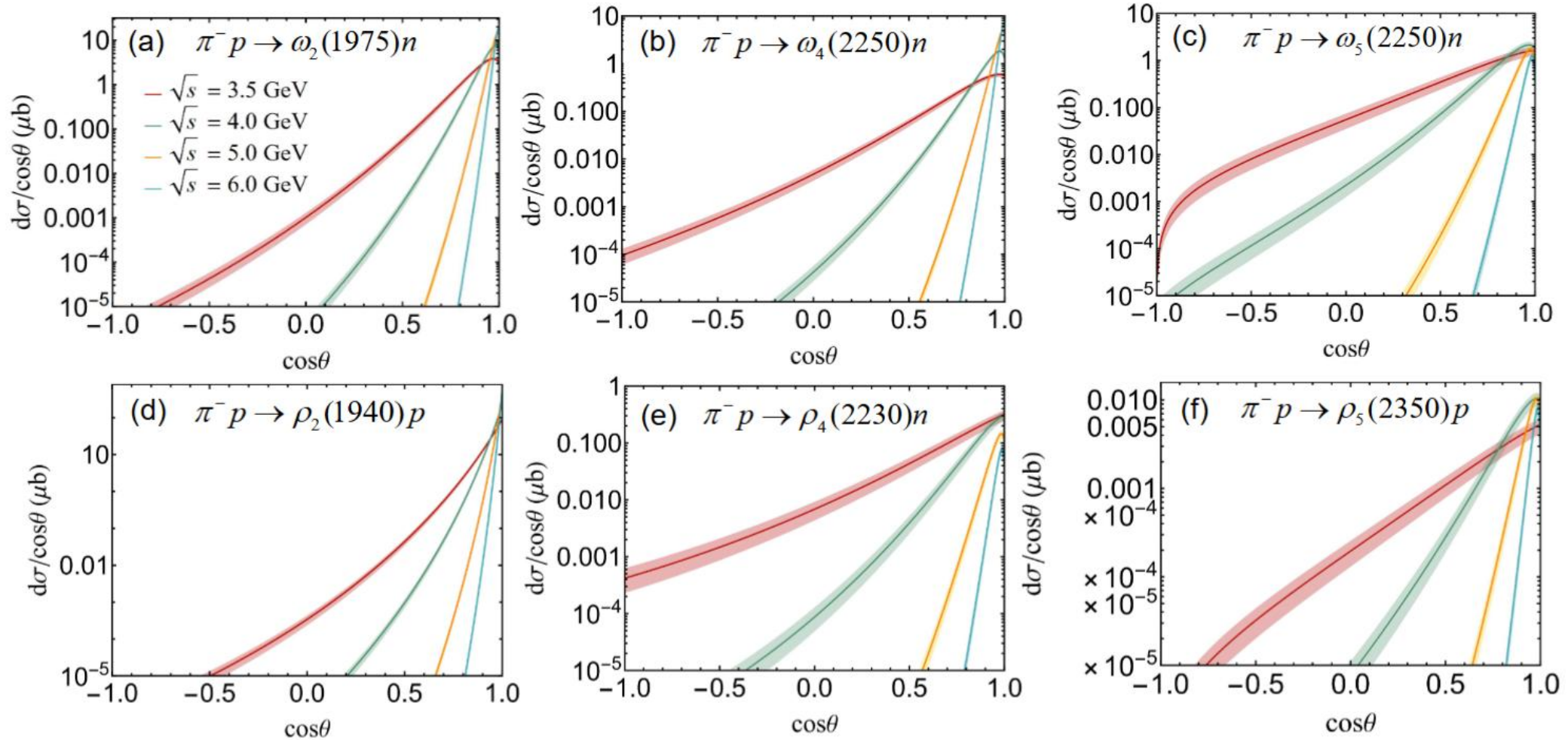


FIG. 9: The differential cross section $d\sigma/d\cos\theta$ of the $\omega_2(1975)$, $\rho_2(1940)$, $\omega_4(2250)$, $\rho_4(2230)$, $\omega_5(2250)$, $\rho_5(2350)$ production at different c.m. energies $W = 3.5, 4, 5$ and 6 GeV.

Possible future prospect

图片取自 刘翔教授 在“第八届强子谱和强子结构研讨会”的报告PPT

- The experimental data for two types of mesons were fitted **using the same cutoff** parameter.
- The production of six high-spin particles was predicted **under the same production mechanism**.
- **Given the secondary decay channels**. Experimentally, these high-spin particles can be **reconstructed** via their invariant mass spectra.



Thank you

从“已知”中提炼“未明”